

# W H E N I S A S E M I C L A S S I C A L A P P R O X I M A T I O N S E L F - C O N S I S T E N T ?

Suzhou Huang  
Center for Theoretical Physics  
Laboratory for Nuclear Science  
and Department of Physics  
Massachusetts Institute of Technology  
Cambridge, Massachusetts 02139  
(hep-ph/9605461. May 1996)

## Abstract

A general condition for the self-consistency of a semiclassical approximation to a given system is suggested. It is based on the eigenvalue distribution of the relevant Hessian evaluated at the stream line configurations (configurations that almost satisfy the classical equations of motion). The semiclassical approximation is consistent when there exists a gap that separates small and large eigenvalues and the spreading among the small eigenvalues is much smaller than the gap. The idea is illustrated in the case of the double-well potential problem in quantum mechanics. The feasibility of the present idea to test instanton models of QCD vacuum is also briefly discussed.

Submitted to: Physical Review D

Typeset using REVTeX

# I. INTRODUCTION

Identification of the most important degrees of freedom in a complicated physics process is often desirable and instructive. This identification is particularly simple when a scale separation exists in the problem under consideration. The energy gap, which divides the degrees of freedom into light and heavy (or sometimes called slow and fast) modes, is a necessary condition for such an endeavor to be successful.

The semiclassical approximation is one of the widely used technique in achieving the isolation of the relevant degrees of freedom. Here we limit the term semiclassical approximation to the expansion of functional integrals around classical saddle point (or generically called instantons). A natural question coming to mind is how the scale separation manifests in this type of approximations. This question is easily answered in the classical limit. In the context of the saddle point expansion the relevant scale is set by the eigenvalues of the Hessian evaluated at the saddle point. The Hessian here is defined as the second derivative of the action with respect to the functional integration variable evaluated at the saddle:  $S^{(0)}[\text{saddle}](x;y) = \frac{1}{2} S''[\text{saddle}](x)(y)$ , where  $\text{saddle}$  satisfies the classical equation of motion  $S'[\text{saddle}](x) = 0$ .

For theories without scale invariance, such as the one dimensional double-well potential problem, the light modes are the zero modes arising for symmetry reasons. The other non-vanishing eigenvalues, separated by some intrinsic scale of the theory from the zero modes, correspond to the heavy modes. As long as the coupling remains small, which in turn ensures the diluteness of the instanton ensemble, this picture is generally preserved. Under this circumstance identifying the collective motion of the nearly zero modes as the relevant degrees of freedom is obvious.

For other theories, such as the two dimensional  $O(3)$  non-linear  $\sigma$ -model and the four dimensional  $SU(N)$  Yang-Mills theory, it is also possible to find modified Hessians such that the eigenvalue spectra evaluated at isolated instanton backgrounds have gaps that separate the zero modes from non-zero modes. The modified Hessians are actually defined by using non-trivial space-time integration measures; in general these measures transform the continuous spectra of the naive Hessians into discrete spectra by compactifying the space-time volume. In the two dimensional  $O(3)$  non-linear  $\sigma$ -model, the modified Hessian shares the same eigenvalue spectrum with the naive Hessian for an isolated instanton [1]. In contrast, the spectrum of the modified Hessian in the four dimensional  $SU(N)$  Yang-Mills theory becomes discrete, whereas the naive Hessian has a continuous spectrum in the dilute limit [2]<sup>1</sup>. In the remaining part of this paper the word Hessian always refers to the one whose eigenvalue spectrum is discrete and has an explicit gap in a single instanton background.

However, the scale invariance of these theories can make the eigenvalue gap arbitrarily small even in the best cases. In fact the eigenvalues are proportional to  $\frac{1}{\rho^2}$ , where  $\rho$  is the size parameter of the instanton. The size parameter in a scale invariant theory, as well as the diluteness, cannot be controlled externally, but are determined only by the specific dynamics. Therefore, it is not obvious that the collective motions of the nearly zero modes

---

<sup>1</sup>I thank Ian Balitsky for reminding me the latter fact.

are the dominant configurations. In light of the lack of a systematic and analytic method in analyzing these situations, we have no alternative but to resort to numerical approaches.

In this paper we propose to explicitly examine the eigenvalue distribution of the Hessian evaluated at the so-called stream line configurations numerically. The concept of stream lines was originally introduced in the context of semiclassical approximation in [3]. The precise definition of the stream line in our numerical work is not too important. Roughly speaking, stream lines are smooth configurations that almost satisfy the classical equation of motion; the corresponding Hessians possess parametrically small or even negative eigenvalues, which would be zero modes in the dilute limit. As pointed out in [3], although they are generally not zero modes, the stream lines can not be treated as Gaussian modes in the functional integration, but rather should be regarded as part of the collective modes.

In practice, we obtain the stream lines from the thermalized configurations by locally minimizing the action or cooling. Therefore, a quantitative understanding of cooling is essential. In section II we present a linearized theory of cooling based on the eigenvalue structure of the Hessian. Then, we argue that the consistency of the semiclassical approximation relies on the fact that there exists a window in cooling time where the eigenvalue distribution of the corresponding Hessian has the properties: i) there is a gap that divides all eigenvalues into small and large ones; and ii) the spreading among the small eigenvalues is small relative to the gap. Correlating the information of the eigenvalue distribution with the monitoring of the physical observable of interest as a function of cooling time will enable us to unambiguously identify whether the instanton ensemble is relevant to the particular physical observable under consideration. As we will see, condition i) is to guarantee that the large eigenmodes can be integrated out perturbatively; and condition ii) is to guarantee that cooling does not distort too much the small eigenmodes. In section III, we explicitly demonstrate this idea in the one-dimensional quantum mechanical problem of the double-well potential.

Of course, any configuration will reach a dilute instanton plateau if cooled long enough, independently of the initial condition. This is why we have to correlate the information of the eigenvalue distribution with the monitoring of the physical observables of interest. Only when the measurement of the interested physical observables is insensitive to the cooling within the cooling window mentioned above the information from the eigenvalue distribution is truly relevant. Physically, the conditions on the Hessian eigenvalues only guarantee that it is possible to separate slow and fast modes (by cooling for instance), but we also need to make sure that the specific observable be dominated by these slow modes.

It is also important to keep in mind that the stream line configurations should not be regarded as some kind of approximation to the original thermalized configurations. Instead, the stream line configuration is only used as a point in function space at which the semiclassical expansion is performed, or about which the full theory can be possibly linearized. For example, it would not be appropriate to assume in general that the topological charge susceptibility measured using the stream line configurations be the true topological charge susceptibility.

Finally, since our ultimate interest is to test various instanton models of QCD vacuum, we will briefly discuss the feasibility of the method proposed here in section IV. In addition, we also speculate on how the sizes of the gap and the spreading of the would-be zero modes are related to the average instanton size and inter-instanton distance used in QCD phenomenology.

Even though cooling is used to obtain the stream line configurations, there is nothing special or unique about this technique. In fact, the precise location of the stream lines in functional space is not too restrictive. We show in the Appendix that almost identical stream lines can be obtained by using the neural network technique, often employed in the usual image processing, in the quantum mechanics example with a double-well potential.

## II. A LINEARIZED THEORY OF COOLING

Since the stream line configurations are obtained from the thermalized ones by using cooling, it is crucial to understand, at least at a semi-quantitative level, what cooling is actually doing to configurations. For simplicity we will use the continuum notations in this section, because the concept is also valid in the continuum. The generalization to lattice formulation is straightforward.

The stream line configurations are obtained from the thermalized configurations by locally minimizing the action or cooling with the relaxation equation, following the direction of the classical force,

$$\frac{\partial \varphi_t(\mathbf{x})}{\partial t} = - \frac{S[\varphi_t]}{\varphi_t(\mathbf{x})}; \quad (1)$$

where the subscript  $t$  labels the cooling time and the initial configuration  $\varphi_{t=0}(\mathbf{x})$  is already in thermal equilibrium. One can easily recognize that the above equation is the Langevin equation [4] with the white noise switched off. After certain period of cooling the configuration becomes smooth and almost satisfies the classical equation of motion. At this point (say at  $t = t_0$ ) the force term,  $S[\varphi_{t_0}]$ , is small and hence the configuration can be regarded as a stream line, which we call  $\varphi_{t_0}(\mathbf{x})$ .

In general, Eq.(1) is difficult to solve, though sometimes numerically tractable. In order to have an analytic understanding let us linearize the force term near the stream line, i.e.  $S[\varphi_t] \approx S[\varphi_{t_0}] + \langle \varphi_t - \varphi_{t_0} | S^{(0)}[\varphi_{t_0}] | \varphi_t - \varphi_{t_0} \rangle$ . This approximation is of course equivalent to approximating the action as

$$S[\varphi_t] \approx S[\varphi_{t_0}] + \langle \varphi_t - \varphi_{t_0} | S^{(0)}[\varphi_{t_0}] | \varphi_t - \varphi_{t_0} \rangle + \frac{1}{2} \langle \varphi_t - \varphi_{t_0} | S^{(0)}[\varphi_{t_0}] | \varphi_t - \varphi_{t_0} \rangle; \quad (2)$$

where  $\langle \cdot | \cdot \rangle$  denotes the scalar product in  $\mathbf{x}$ -space. How good is this linear approximation in fact strongly correlates with how well the system can be treated semiclassically.

The linearized Eq.(1) can be trivially solved by finding the eigenvalues and eigenvectors of the Hessian  $S^{(0)}[\varphi_{t_0}]$ ,

$$\sum_{\mathbf{y}} S^{(0)}[\varphi_{t_0}](\mathbf{x}; \mathbf{y}) \varphi_{\mathbf{y}} = \lambda_{\mathbf{l}} \varphi_{\mathbf{l}}(\mathbf{x}); \quad (3)$$

The eigenvalue label  $\mathbf{l}$  can be either discrete or continuous in general. Expanding  $\varphi_t(\mathbf{x})$  and  $S^{(0)}[\varphi_{t_0}](\mathbf{x})$  in terms of the complete basis  $f_{\mathbf{l}}; \varphi_{\mathbf{l}}(\mathbf{x})$ ,

$$\varphi_t(\mathbf{x}) - \varphi_{t_0}(\mathbf{x}) = \sum_{\mathbf{l}} c_{\mathbf{l}}(t) \varphi_{\mathbf{l}}(\mathbf{x}) \quad \text{and} \quad S^{(0)}[\varphi_{t_0}](\mathbf{x}) = \sum_{\mathbf{l}} f_{\mathbf{l}} \varphi_{\mathbf{l}}(\mathbf{x}); \quad (4)$$

the linearized version of Eq.(1) can be immediately integrated, yielding

$$c_1(t) = c_1(0) e^{-\gamma_1 t} \frac{f_1}{\gamma_1} + e^{-\gamma_1 t} : \quad (5a)$$

Since we are expanding around stream lines and hence  $f_1$ 's are generally small, Eq.(5a) would be always dominated by the first term unless when  $\gamma_1 \neq 0$ . In the latter case, Eq.(5a) becomes

$$c_1(t) = c_1(0) + f_1 t \quad \text{when } \gamma_1 \neq 0 : \quad (5b)$$

Therefore, the eigen modes can be classified according to the magnitudes of their eigenvalues. When the eigen mode obeys Eq.(5a) with the first term being dominating (or in the subspace  $\gamma_1 < 0$ ), the corresponding coefficient of  $\phi_1(x)$  is being damped (or magnified when  $\gamma_1 < 0$ ) by the factor  $\exp(-\gamma_1 t)$ . On the other hand, when the eigen mode obeys Eq.(5b) (or in the subspace  $\gamma_1 \neq 0$ ), the corresponding coefficient of  $\phi_1(x)$  is being drifted by the classical force  $f_1$ . It is natural to identify the subspace of  $\gamma_1 < 0$  as Gaussian fluctuations and the subspace of  $\gamma_1 \neq 0$  as collective motions.

Now we explicitly see why we need the existence of a gap in the eigenvalue distribution and why we need the eigenvalue spreading near zero to be small relative to the gap. The first condition guarantees that the Gaussian fluctuation can be safely treated perturbatively. The second condition guarantees that cooling can be used effectively in practice to filter out the Gaussian fluctuation without distorting too much the collective coordinates. The spreading among the small eigenvalues, in fact, serves as a measure of the strength of the inter-instanton interaction.

It should be recognized that the eigen basis  $\phi_1; \phi_2(x)g$  is  $t_0$  dependent, through the dependence of the stream line solution  $\phi_0(x)$  in the definition of the Hessian  $S^{(0)}[t_0]$ . However, this dependence is very mild if those two conditions in the eigenvalue distribution are satisfied. In other words, there should be a window in  $t_0$  such that the eigen basis  $\phi_1; \phi_2(x)g$  is rigid and almost independent of the precise location of  $t_0$ . One of course in principle can expand  $\phi_t(x)$  around any complete set. The specialty about the stream line  $\phi_0(x)$  is that the quadratic approximation Eq.(2) is more likely to work than an arbitrary set, in the sense that  $f_1$ 's and  $c_1(0)$ 's are small, and hence the drifting forces and anharmonic terms are ignorable.

Due to the interaction between instantons (even at the classical level), the force term never exactly vanishes and some of the eigenvalues can be slightly negative. Therefore, the stream line configurations are only metastable with respect to cooling. To what extent cooling can isolate a stream line configuration in fact also crucially depends on whether the gap in the eigenvalue distribution of the Hessian exists and on whether the eigenvalue spreading near zero is smaller than the gap. This seemingly disadvantageous property actually provides us a nice diagnosis for the self-consistency.

Finally, it should be emphasized that eigenvalue distribution of the Hessian is actually intrinsic, not necessarily only pertinent to the interpretation of cooling. For example, conditions i) and ii), when satisfied, will be reflected from the Monte Carlo dynamics (at least for local updates) by showing two characteristic auto-correlation time scales, given by the inverses of the gap and the spreading.

### III. THE DOUBLE-WELL POTENTIAL PROBLEM

In this section we explicitly illustrate the idea outlined earlier in the problem of the one dimensional double-well potential in quantum mechanics, defined by the Hamiltonian

$$\hat{H} = \frac{1}{2} \frac{d^2}{dx^2} + V(x) \quad \text{with} \quad V(x) = \frac{g^2}{2} x^2 - \frac{1}{4g^2} x^4; \quad (6)$$

In terms of the path integral formulation the corresponding Euclidean action in a finite box of length  $L$  is given by

$$S[x] = \int_0^L dx \left[ \frac{1}{2} \left( \frac{dx}{dx} \right)^2 + \frac{g^2}{2} x^2 - \frac{1}{4g^2} x^4 \right]; \quad (7)$$

The energy level splitting between the first excited state and the ground state as a function of the coupling constant,  $E(g) = E_1(g) - E_0(g)$ , is the primary concern here. The nice feature of this problem is that instanton density can be systematically controlled by dialing the coupling constant. Hence we know whether the semiclassical picture is good or bad at a given coupling.

#### A. Known results

The physics associated with  $E(g)$  is well known [5]. In the weak coupling limit ( $g$  small)  $E(g)$  is dominated by the dilute instanton configurations or the tunneling effect. In this regime the semiclassical approximation is expected to be good. As the coupling  $g$  increases, the instanton density also increases. The interaction between near-by instantons and other long wavelength objects, such as the ucton introduced in [6], become important. Then we expect that the semiclassical approximation fails in the strong coupling regime. We would like to verify that the eigenvalue distribution of the Hessian evaluated in the stream line configurations can tell us for what values of  $g$  the semiclassical approximation is reliable.

To have a quantitative idea on where the semiclassical approximation is valid we quote the perturbative (around one instanton) result up to three loops [7,8] for  $E(g)$

$$E(g) = \frac{2}{g^2} \exp \left[ -\frac{1}{6g^2} \right] \left[ 1 - \frac{71}{12} g^2 - \frac{315}{8} g^4 + O(g^6) \right]; \quad (8)$$

which is plotted in Fig.1. For comparison, the exact numerical result, calculated using the method of moments recursion [9], is also included. Because the perturbative expansion is divergent and non-Borel summable, the perturbative result quickly deteriorate at  $g > 0.25$ . Therefore,  $g = 0.25$  can be regarded as a rough division between the weak and strong coupling regimes. A similar value of  $g$  can also be estimated by requiring that the average distance between nearby instantons be comparable with the instanton size (in the weak coupling limit the instanton density  $\propto E(g)$ ).

It is also useful to list the known properties of a well isolated instanton in this theory. The continuum instanton solution is given by  $\phi_{\text{instanton}}(x) = \frac{1}{2g} \tanh\left(\frac{x}{2}\right)$  and the associated action

is  $S_0 = 1/(6g^2)$ . The eigenvalue problem of the Hessian in the background of  $\phi_{\text{kink}}(\mathbf{x})$  is equivalent to a one dimensional Schrodinger equation with a potential  $V^0(\phi_{\text{kink}}(\mathbf{x}))=2$

$$-\frac{1}{2} \frac{d^2}{dx^2} + 3g^2 \phi_{\text{kink}}^2(\mathbf{x}) - \frac{1}{4} \phi(\mathbf{x}) = -\epsilon_l \phi(\mathbf{x}); \quad (9)$$

where  $\epsilon_l$  labels eigenvalues. The solution of this equation has been worked out long time ago [10]. There are two bound states with  $\epsilon_0 = 0$ , corresponding to the so-called translation zero mode (with  $\phi_0(\mathbf{x}) \propto \phi'_{\text{kink}}(\mathbf{x})$ ), and  $\epsilon_1 = 3/8$ , followed by a continuum with a threshold  $\epsilon_c = 1/2$ . These features will be recognized later from the eigenvalue distribution of the Hessian in the weak coupling regime. Since there is no scale invariance in this model, the size of the instanton is fixed.

## B. Numerical results

The thermalized configurations are generated by the standard Metropolis method [11], accompanied by the embedded cluster updating of [12]. Without the embedded cluster updating it would take too long to have a good sampling of the action in the weak coupling regime. For our purpose it is sufficient to use the simplest lattice action

$$S_L[\phi] = a^4 \sum_{n=1}^N \left[ \frac{1}{2} \left( \frac{\phi(n+1) - \phi(n)}{a} \right)^2 + \frac{g^2}{2} \phi^2(n) - \frac{1}{4g^2} \phi^4(n) \right]; \quad (10)$$

where  $a$  is the lattice spacing and  $N = L/a$ . It is easy to verify that the lattice action for a single instanton is related to its continuum counterpart by  $S_0^L = S_0 = 1 + a^2/360 + O(a^4)$ . Therefore, as long as  $a < 1$  the discretization error is under control. In the simulation  $N$  has to be sufficiently large to ensure that enough instantons are present in each thermalized configuration. As mentioned earlier, the instanton density is equal to  $E(g)$  in the weak coupling limit. So we have chosen  $L = E(g) > 10$ , which translates into  $N$  ranging from 200 to 500 for the various  $g$ 's we have considered. For such big values of  $N$  the boundary effect is irrelevant, and we choose the periodic boundary condition for simplicity.

In the Monte Carlo simulation, one iteration is defined as a Metropolis sweep plus a embedded-cluster sweep. Typically, 500 iterations are used to thermalize an arbitrary initial configuration. Then 1000 independent configurations, separated by 50 iterations, are used in the measurement in all cases considered.

Physical observables are measured as follows. The ground state energy can be calculated using the Virial theorem

$$E_0(g) = \frac{D}{2} \langle V^0(\phi) \rangle + \frac{E}{2} \langle \phi^4(\phi) \rangle; \quad (11)$$

The ground state wavefunction squared  $\phi_0^2(\phi)$  can be obtained by histogramming the Monte Carlo history of  $\phi(\mathbf{x})$  after thermalization. The energy splitting between the ground state and the first excited state can be read off from the exponential decay of the two-point correlation function at large  $|\mathbf{x}-\mathbf{y}|$

$$\langle \phi(\mathbf{x}) \phi(\mathbf{y}) \rangle \sim \exp(-E(g)|\mathbf{x}-\mathbf{y}|); \quad (12)$$

The stream line configurations are obtained from the thermalized configurations by locally minimizing the action iteratively or cooling,

$$\phi_{t+1}(n) = \phi_t(n) - \frac{2\phi_t(n) - \phi_t(n+1) - \phi_t(n-1)}{a} + 2ag^2 \phi_t(n)^h \phi_t(n)^2 - \frac{1}{4g^2} ; \quad (13)$$

a discretized version of Eq.(1). The above iteration is implemented in the serial mode (or parallel mode with checkerboard) to avoid numerical instability. This implies that the cooling speed does not exactly obey the analysis in the previous section, which holds strictly in the parallel (without checkerboard) mode. The instability in the parallel mode is due to the fact that those modes with negative eigenvalues get magnified under Eq.(13). A value of  $\epsilon = 0.1$  is found to be adequate in our study. Violation of the classical equation of motion can be monitored from the first derivative of the lattice action  $S_L^0[\phi_t]$

$$f[\phi_t(n)] = \frac{S_L^0[\phi_t(n)]}{a} = \frac{2\phi_t(n) - \phi_t(n+1) - \phi_t(n-1)}{a^2} + 2g^2 \phi_t(n)^h \phi_t(n)^2 - \frac{1}{4g^2} : \quad (14)$$

The following mean value (relative to the location of the classical vacua) is defined, which can serve as a quantitative measure of the violation of the classical equation of motion on average

$$\bar{f} = \frac{2g}{N} \sum_{n=1}^N f[\phi_t(n)] : \quad (15)$$

### 1. An idealized case

The stream line solution in an idealized case, a near-by instanton and anti-instanton pair, has been studied some time ago in [6]. We add to that study by explicitly solving also the eigenvalues and eigenvectors of the associated Hessian. In Fig 2(a) we show the stream line solution of a slightly overlapped instanton and anti-instanton pair (heavy dots), the corresponding violation of the classical equation of motion (solid line) and the two eigenvectors with the lowest eigenvalues,  $\lambda^+ = 0.025041$  (dashed line) and  $\lambda^- = 0.004947$  (dash-dotted line), respectively. Other eigenvalues are 0.308339 or higher. The separation of the instanton and anti-instanton is roughly 6, while the "radius" of an instanton is about 3 (or a full size of about 6). The violation of the classical equation of motion is hardly noticeable. If the instanton and anti-instanton were widely separated the two lowest eigenvalues would both be vanishing and the gap would be exactly  $\lambda_1 = \lambda_2 = 0.375$ . Of course, a slight overlap lifts the degeneracy. The total action of this stream line is  $1.9683S_0$ .

Notice that one of the eigenvalue is still close to zero, corresponding to the translation of the instanton and anti-instanton pair together. The other eigenvalue becomes noticeably negative, due to the attraction between the instanton and anti-instanton, corresponding to the relative motion between the two objects. The minus sign of the lowest eigenvalue implies that the system is not stable under cooling and the instanton and anti-instanton eventually annihilate each other. However, because  $\lambda^+ + \lambda^-$  is much smaller than the gap, it is possible to find a cooling-time window such that the higher modes are strongly damped while the pair is still almost intact. In the actual configuration the spread of the small eigenvalues



relative to the gap is a very good indicator whether cooling is capable of faithfully separating collective modes from Gaussian modes, or more precisely whether these two sets of modes can be defined in a meaningful way.

When instanton and anti-instanton are closer, the violation of classical equation of motion gets larger and the eigenvalue structure become very different from the dilute limit. In Fig 2 (b), a pair with separation comparable to the radius of instanton is displayed. Now the lowest four eigenvalues are 0.137194, 0.116332, 0.379692 and 0.501244. In this case, the gap is about only 3 times larger than the spreading of the two small eigenvalues, and the total action is  $1.4628S_0$ . In this case the trace of instanton and anti-instanton is marginally identifiable.

In Fig.3 the lowest ten eigenvalues are plotted as functions of the instanton and anti-instanton separation  $s$ . When  $s$  is large the pattern of the eigenvalues are verified as that of the weak coupling limit. When  $s$  becomes comparable with the instanton size the lowest four eigenvalues start to deform, while the higher eigenvalues stay more or less the same. When  $s$  is smaller than the radius of the instanton the eigenvalue pattern reduces to that of the zero background field or the plane waves.

## 2. A weak coupling case

The weak coupling case we considered involves the following parameters:  $g = 0.20$ ,  $a = 0.4$  and  $L = 200$  (or  $N = 500$ ). Before cooling ( $N_{\text{cool}} = 0$ ) we measured the following quantities. From Eq.(11) the ground state energy  $E_0 = 0.415(3)$ , whose corresponding wavefunction squared is shown as a dashed line in Fig.4 (a)). The two-point function is shown in Fig.4 (b)) as dots (lower curve); from the values of the two-point function in the interval  $x \in (6; 30)$  and Eq.(12) we extracted the energy splitting  $E^{(0)} = 0.060(2)$ . For comparison, the exact ground state energy and the energy gap at the same coupling are:  $E_0^{(\text{exact})} = 0.4198$  and  $E^{(\text{exact})} = 0.0609$ .

A typical configuration at  $N_{\text{cool}} = 50$  is depicted by open dots in Fig.4 (c). It is easily recognized that this configuration is a dilute superposition of instantons and anti-instantons. The violation of classical equation of motion is small ( $f = 0.02442$ ), as indicated by the thin line in Fig.4 (c). Therefore, the configurations after  $N_{\text{cool}} = 50$  sweeps of cooling are good candidates of stream lines. At  $N_{\text{cool}} = 50$  we present the two-point function in Fig.4 (b) with crosses (upper curve) and the eigenvalue distribution of the Hessian with a thick-line histogram in Fig.4 (d). To make sure that the cooling window indeed exists we also calculated the two-point function (middle curve with open dots in Fig.4 (b)) and the eigenvalue distribution of the Hessian (thin line in Fig.4 (d)) at  $N_{\text{cool}} = 25$ . A comparison of the results at two different values of cooling sweep gives us some idea on the evolution of these quantities as functions of cooling time.

Since we are in the weak coupling regime, Fig.4 (d) clearly show the anticipated properties: i) the existence of a gap that separates small and large eigenvalues and ii) the spreading among the small eigenvalues is small relative to the gap. Various peaks in this figure can be easily identified. The peak near  $\lambda = 0$  is associated with the "would-be" zero-modes, with an effective width less than 0.1. The peak near  $\lambda = 0.35$  is associated with the second discrete level mentioned in the last subsection. The third peak represents the onset of the

continuum at  $\beta = 0.5$ . The effective gap can be roughly estimated to be between 0.35 to 0.5.

Fitting the cooled two-point functions with Eq.(12) for  $x$  in the interval (6;30), we obtain  $E^{(25)} = 0.061(2)$  and  $E^{(50)} = 0.057(2)$  for  $N_{\text{cool}} = 25$  and  $N_{\text{cool}} = 50$ , respectively. These two numbers agree with the uncooled result within statistical errors, as it is also visually seen in Fig.4 (b) being the three curves nearly parallel. The measured ground state energy with these stream lines at  $N_{\text{cool}} = 25$  and  $N_{\text{cool}} = 50$  are very small, not surprisingly, since we do not expect the ground state energy be dominated by the instanton physics. Correlating the informations from Fig.4 (b) and Fig.4 (d) we can safely conclude that the energy splitting  $E$  at  $g = 0.20$  is dominated by the dilute instanton physics, and hence can be self-consistently treated semiclassically.

### 3. A strong coupling case

The strong coupling case we considered involves the following parameters:  $g = 0.50$ ,  $a = 0.2$  and  $L = 40$  (or  $N = 200$ ). Before cooling ( $N_{\text{cool}} = 0$ ) we measured the following quantities. From Eq.(11) the ground state energy  $E_0 = 0.293(5)$ , whose corresponding wavefunction squared is shown as a dashed line in Fig.5(a)). The two-point function is shown in Fig.5(b)) as dots (lower curve); from the values of the two-point function in the interval  $x \in (0.6;6)$  and Eq.(12) we extracted the energy splitting  $E^{(0)} = 0.643(10)$ . For comparison, the exact ground state energy and the energy splitting at the same coupling are:  $E_0^{(\text{exact})} = 0.2940$  and  $E^{(\text{exact})} = 0.6374$ .

Since we are in the strong coupling region there is no dilute instanton physics associated with the energy splitting  $E$  now. We, therefore, anticipate that the information from monitoring  $E$  and the eigenvalue distribution of the Hessian as functions of cooling time will indicate that the self-consistency of the semiclassical approximation is violated. This expectation is borne out explicitly.

The relevant results are shown in Fig.5, with the same notations as in Fig.4. The energy splittings fitted from data with  $x \in (4;8)$  are  $E^{(25)} = 0.55(2)$  at  $N_{\text{cool}} = 25$ , and  $E^{(50)} = 0.43(2)$  at  $N_{\text{cool}} = 50$ . These values are much lower than the uncooled results, well beyond statistical errors, as can also be seen in Fig.5 (b) where the three sets of data points are no longer parallel. In addition, figure 5 (d) shows that the eigenvalue distribution does not have the two required properties i) and ii) even at  $N_{\text{cool}} = 50$ . In fact, the gap is clearly absent and the eigenvalue spreading of the "would-be" zero modes is large. The absence of a gap and the large spreading of the "would-be" zero modes can also be inferred from a typical configuration after  $N_{\text{cool}} = 50$ . In addition, there are peaks showing up at large  $n$ , whose position coincide with the spectrum of the free Hessian ( $r^2=2$ ):  $\omega_n = [1 - \cos(2\pi n/N)]^{1/2}$ .

From Fig.5 (c) we observe that the violation of the classical equation of motion is large ( $f = 0.09246$ ). Although the cooled configuration is smooth, it is not a superposition of dilute instantons and anti-instantons. This means that the theory cannot be linearized around this kind of stream lines of poor quality. Even if one insists that this kind of configurations be treated as stream lines, the force terms would be so large that these stream lines would interact strongly, hence a self-consistency could not be sustained. So we conclude that, for  $g > 0.5$ , there is no meaningful separation of collective modes from Gaussian fluctuations.

One could argue that the energy splitting can always be measured at asymptotically large distances, even after many but fixed number of cooling sweeps, since a finite number of cooling sweeps would not modify correlations at distances much larger than the number of cooling sweeps times the lattice constant. However, the real relevant question is whether the energy splitting can be extracted at a distances of the order of  $l = E$  right after the further excited states are damped out. In the weak coupling case, we see that the window in  $x$  used to extract  $E$  is very much the same before and after cooling. In contrast, a similar window does not exist in the strong coupling case. The cooled two-point functions do not even display clean exponential behavior till  $x > 4$  or more.

#### 4. An intermediate coupling case

The intermediate cooling case we considered involves the following parameters:  $g = 0.35$ ,  $a = 0.2$  and  $L = 40$  (or  $N = 200$ ). Before cooling ( $N_{\text{cool}} = 0$ ) we measured the following quantities. From Eq.(11) the ground state energy  $E_0 = 0.283(4)$ , whose corresponding wavefunction squared is shown as a dashed line in Fig.6(a)). The two-point function is shown in Fig.6(b)) as dots (lower line); from the values of the two-point function in the interval  $x \in (0.6; 6)$  and Eq.(12) we extracted the energy gap  $E = 0.399(7)$ . For comparison, the exact ground state energy and the energy gap at the same coupling are:  $E_0^{(\text{exact})} = 0.2852$  and  $E^{(\text{exact})} = 0.3870$ .

Now we are in the intermediate situation. The results, depicted in Fig.6, lie somewhere between the weak and strong coupling cases. The energy splitting fitted from data at  $x \in (4; 8)$  are  $E^{(25)} = 0.36(2)$  ( $N_{\text{cool}} = 25$ ) and  $E^{(50)} = 0.33(2)$  ( $N_{\text{cool}} = 50$ ); both values are slightly lower than the uncooled value. The violation of the classical equation of motion after  $N_{\text{cool}} = 50$  is larger than that of  $g = 0.20$ , but smaller than that of  $g = 0.50$  ( $f = 0.05389$ ). It is interesting to note how the eigenvalue distribution of the Hessian deforms as a function of the coupling  $g$ . First, the peak associated with the "would-be" zero modes seems to be pushed to  $0.15$ . Second, the strength of the peak at the threshold of the continuum (at  $\lambda = 0.5$ ), together with the peak at the second bound state, are now moved to the negative side. A similar type of deformation can also be observed in Fig.5(d). It might not be easy to understand this kind of movement of eigenvalues quantitatively. However, the observed deformation is certainly qualitatively consistent with the attractive nature between instanton and anti-instanton.

#### IV . SUMMARY AND CONCLUSION

We have presented a practical criterion for examining the self-consistency of the semiclassical approach in approximating functional integrals. It is based on the explicit eigenvalue distribution of the Hessian evaluated in stream line configurations. The self-consistency is guaranteed by two conditions: i) there exists a gap that divides eigenvalues into small and large ones; and ii) the spreading among the small eigenvalues is small relative to the gap. We then illustrate how this idea can be explicitly applied in the case of the one dimensional double-well potential problem in quantum mechanics.

It should be noted that conditions i) and ii) do not implies that the dynamics of stream-lines is that of the dilute instanton limit. In general, the dynamics of stream lines are most likely non-trivial. Conditions i) and ii) only guarantees that the separation of the collective motions and the Gaussian fluctuations can be made sensibly.

Of course, the ultimate goal is to apply the same method to QCD, and to establish the self-consistency of the so-called instanton vacuum. Technically, we anticipate no conceptual complications, apart that the definition of the Hessian should be modified as mentioned in the Introduction and that the computation is obviously more demanding. According to [2] the modification of the Hessian requires the knowledge of the location of instantons, which should not be difficult to obtain once we have good candidates of stream line configurations. In addition, the Hessian has similar structure to the Dirac operator, apart from kinematics. It was shown in [2] that the modified Hessian for gluons shares the same eigenvalue spectrum, except multiplicities, as that of the modified Hessian for quarks in the continuum for a single instanton. Since the eigenvalue problem of the lattice Dirac operator is within the reach of today's computational resources, it may not be totally unreasonable to assume that the method proposed here could be applied to the Hessian associated with the gluonic action.

Furthermore, it is well known [2] that the spectrum of the modified Hessian of a well isolated instanton is discrete and the gap is proportional to the inverse of the size parameter squared. For realistic gluon configurations we expect this spectrum to be deformed. To what extent the qualitative behavior of the eigenvalue distribution is preserved will depend on two crucial scales: the average instanton size ( $\bar{\rho}$ ) and the inter-instanton distance ( $R$ ). It is not difficult to imagine that, provided the instanton ensemble is not too dense,  $1/\bar{\rho}^2$  controls the size of the gap, and some positive power of  $1/R$  controls the spreading of the would-be zero modes.

In addition, phenomenologically, we roughly know that instantons play a very important role in low energy light hadronic physics [13]. This phenomenological picture, including the average size of instantons ( $\bar{\rho} \approx 0.3$  fm) and inter-instanton distance ( $R \approx 1.0$  fm), is confirmed to some extent by lattice calculations [14]. An explicit examination of the eigenvalue distribution of the Hessian evaluated at stream line configurations in QCD will give us direct and unambiguous information on how reliable the phenomenological instanton models are.

## V. ACKNOWLEDGMENTS

I would like to thank Ian Balitsky, Richard Brower, Marcello Lissia, John Negele and Kostas Orginos for many useful discussions. This work is supported in part by funds provided by the U.S. Department of Energy (D.O.E.) under cooperative research agreement # DF-FC 02-94ER 40818.

## APPENDIX : STREAM LINE VIA NEURAL NETWORK

In the main text of this paper we used the cooling procedure to obtain the stream line configuration. This is due to the convenience of physical interpretation. In this appendix we

show that almost identical stream line can be obtained by using neural network technique, often employed in usual image processing [15].

The idea is to introduce  $N$  linear units  $i_2(n)$ , whose output represents the smoothed configuration at each lattice site. Then the value of  $i_2(n)$  is obtained by minimizing the following cost function

$$E_{\text{cost}} = \sum_{n=1}^N [h_1(n) - i_2(n)]^2 + \sum_{n=1}^N [h_2(n) - i_2(n+1)]^2 : \quad (\text{A } 1)$$

The first term is to enforce the fidelity of the neural network output to the original configuration  $i_1$ . The second term is a physically motivated bias that constrains the neural network output to be smooth. The relative importance of these two terms is controlled by the parameter  $\lambda$ . Since the cost function  $E_{\text{cost}}$  is quadratic in  $i_2$ 's, the unique minimum is guaranteed. The output  $i_2$ 's at the minimum, once  $\lambda$  is properly chosen, can be regarded as a candidate of the stream line configuration. The minimization can be achieved by using, for example, the standard conjugate gradient method.

In Fig.7 we show a typical configuration (in dots) at  $a = 0.25$  and  $g = 0.25$ . The standard cooling procedure with  $\lambda = 0.1$  and  $N_{\text{cool}} = 10$  yields the thick line, while the neural network smoothing with  $\lambda = 10$  yields the thin line. The difference of the thick line and the thin line is tiny. This result is easy to anticipate, because the gradient descent of Eq.(A 1) with respect to  $i_2$  is very similar to the discrete Langevin equation, Eq.(13).

In general, the value of  $\lambda$  needs to be experimented, just like the choice of  $\lambda$  and  $N_{\text{cool}}$  in the cooling. Obviously, various variations need to be incorporated in order to extend Eq.(A 1) to other theories. More sophisticated neural network techniques involving learning (supervised or unsupervised) can also be imagined. Of course, the drawback of this approach is that the precise physical content is theoretically less transparent.

## REFERENCES

- [1] A . Jevicki, Nucl. Phys. B 127 (1977) 125;  
D . Forster, Nucl. Phys. B 130 (1977) 38.
- [2] G . 't Hooft, Phys. Rev. D 14 (1976) 3432.
- [3] I. I. Balitsky and A . V . Yung, Phys. Lett. B 168 (1986) 113;  
E . V . Shuryak, in \Proc. Conf. on numerical experiments in quantum field theories",  
Am a-Ata, 1985, ed. A . A . Migdal (in Russian).
- [4] G . G . Batrouni, et al, Phys. Rev D 32 (1985) 2736.
- [5] A very good discussion of the double-well potential problem from the semiclassical point  
of view can be found in the book by J. Zinn-Justin, \Quantum Field Theory and Critical  
Phenomena", 2nd edition, Oxford Univ. Press, (1993).
- [6] E . V . Shuryak, Nucl. Phys. B 302 (1988) 621.
- [7] J. Zinn-Justin, J. Math. Phys. 22 (1981) 511;
- [8] C . F . W ohler and E . Shuryak, Phys. Lett. B 333 (1994) 467.
- [9] R . Blankenbecler, T . DeGrand and R . L . Sugar, Phys. Rev. D 21 (1980) 1055.
- [10] R . F . Dashen, B . Hasslacher and A . Neveu, Phys. Rev. D 10 (1974) 4130.
- [11] M . Creutz and B . Freedman, Ann. of Phys. 132 (1981) 427;  
E . V . Shuryak and O . V . Zhirov, Nucl. Phys. B 242 (1984) 393;
- [12] R . C . Brower and P . Tamayo, Phys. Rev. Lett. 62 (1989) 1087.
- [13] For existing literature on the instanton models of the QCD vacuum , see E . V . Shuryak,  
Rev. Mod. Phys. 65 (1993) 1; and a forthcoming review article by T . Shafer,  
E . V . Shuryak and J. J. M . Verbaarschot.
- [14] M . Chu and S . Huang, Phys. Rev. D 45 (1992) 2446.  
M . Chu, J. G randy, S . Huang and J. Negele, Phys. Rev. D 49 (1994) 6039.
- [15] see for example, J. Hertz, A . Krogh and R . G . Palmer, \Introduction to the Theory of  
Neural Computation", Addison-W esley (1991), Reading, M ass.

## FIGURES

FIG .1. Energy gap between the first excited state and the ground state as a function of the coupling  $g$ . The solid line is the exact result. The dotted, dot-dashed and dashed lines are the one-loop, two-loop and three-loop perturbative (around a single instanton) results.

FIG .2. (a) Slightly overlapping instanton and anti-instanton and (b) strongly overlapping instanton and anti-instanton pairs. The heavy dots are  $\psi_{\text{pair}}(x)$  at  $g = 0.5$  and  $a = 0.2$ . The solid line is the force term  $S^0[\psi_{\text{pair}}](x)$ . The dashed and dot-dashed lines are the lowest and second lowest eigenvectors of  $S^0[\psi_{\text{pair}}](x; y)$  respectively. The thin dotted lines indicate the two potential minima.

FIG .3. The lowest 10 eigenvalues of the Hessian as a function of the instanton and anti-instanton separation. When the separation is comparable with the instanton size ( $\approx 6$ ) the eigenvalue pattern starts to deviate from the dilute limit.

FIG .4. A weak coupling case:  $g = 0.20$ ,  $a = 0.4$  and  $L = 200$ . (a) ground state wavefunction squared  $\psi_0^2(x)$  at  $N_{\text{cool}} = 0$  (dashed line) and  $N_{\text{cool}} = 25$  (solid line); (b) two-point correlation function  $\langle \psi(x) \psi(0) \rangle$  at  $N_{\text{cool}} = 0$  (lower curve of filled dots),  $N_{\text{cool}} = 25$  (middle curve of open dots) and  $N_{\text{cool}} = 50$  (upper curve of crosses). The errors are purely statistical. When not shown the errors are smaller than symbols; (c) a typical field configuration at  $N_{\text{cool}} = 50$  (open dots), the violation of the classical equation of motion (thin solid line) and the locations of the classical action minima (dashed lines); (d) eigenvalue distribution of the Hessian evaluated at the stream lines  $P(x)$  at  $N_{\text{cool}} = 25$  (thin line) and  $N_{\text{cool}} = 50$  (thick line).

FIG .5. A strong coupling case:  $g = 0.50$ ,  $a = 0.2$  and  $L = 40$ . Notations are the same as that of FIG .4.

FIG .6. An intermediate coupling case:  $g = 0.35$ ,  $a = 0.2$  and  $L = 40$ . Notations are the same as that of FIG .4.

FIG .7. A typical configuration (in dots) at  $a = 0.25$ ,  $g = 0.25$  and  $L = 100$ . The standard cooling with  $\epsilon = 0.1$  and  $N_{\text{cool}} = 10$  yields the thick line. The neural network smoothing with  $\epsilon = 10$  yields the thin line, which is almost indistinguishable from the thick line.

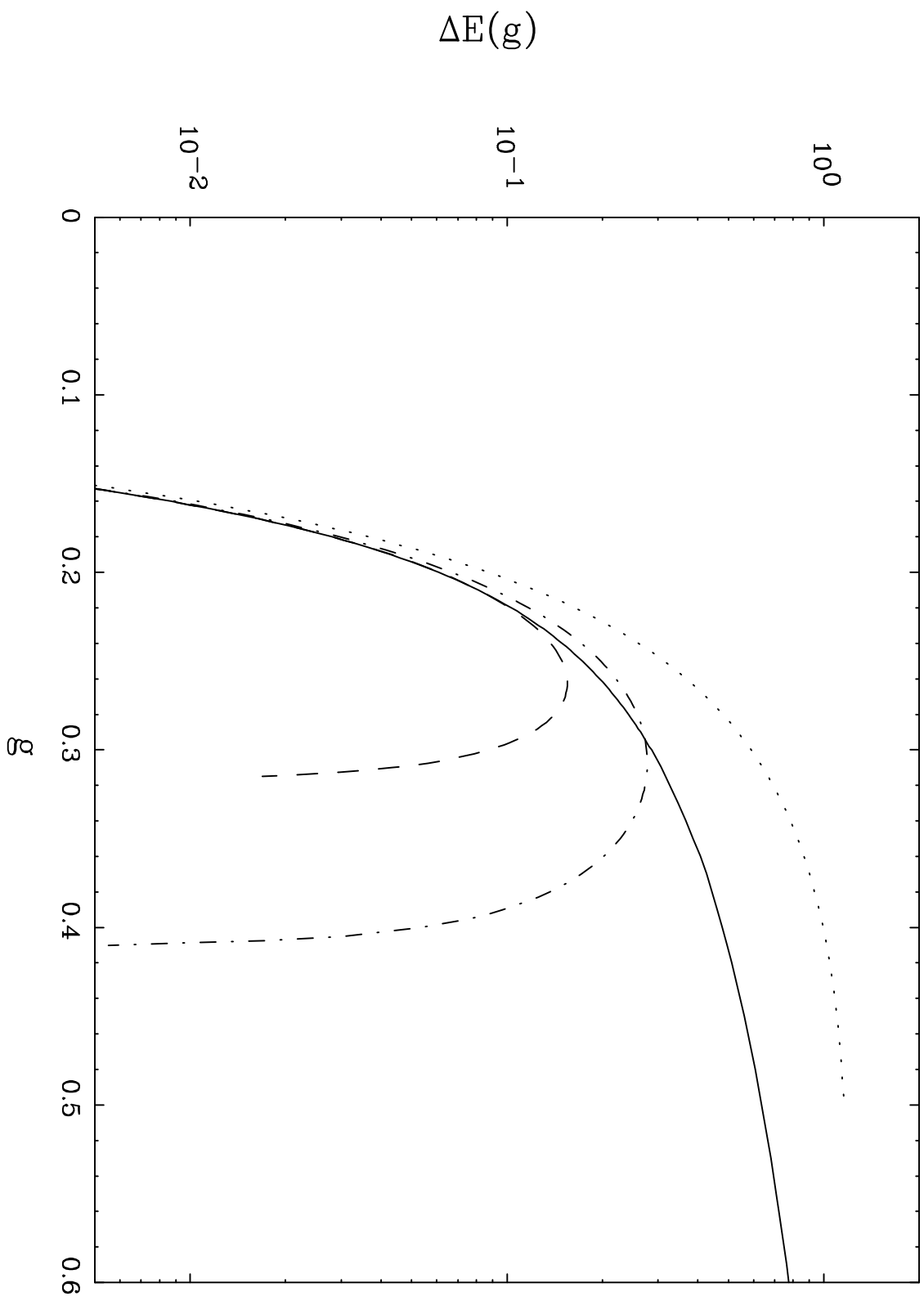


Fig.1



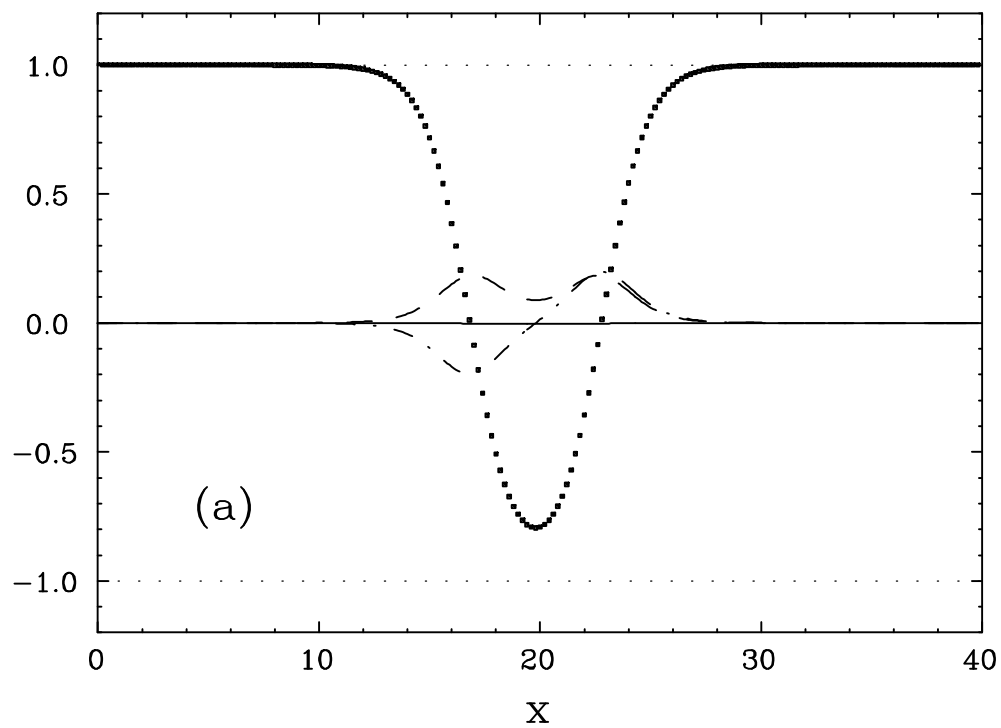
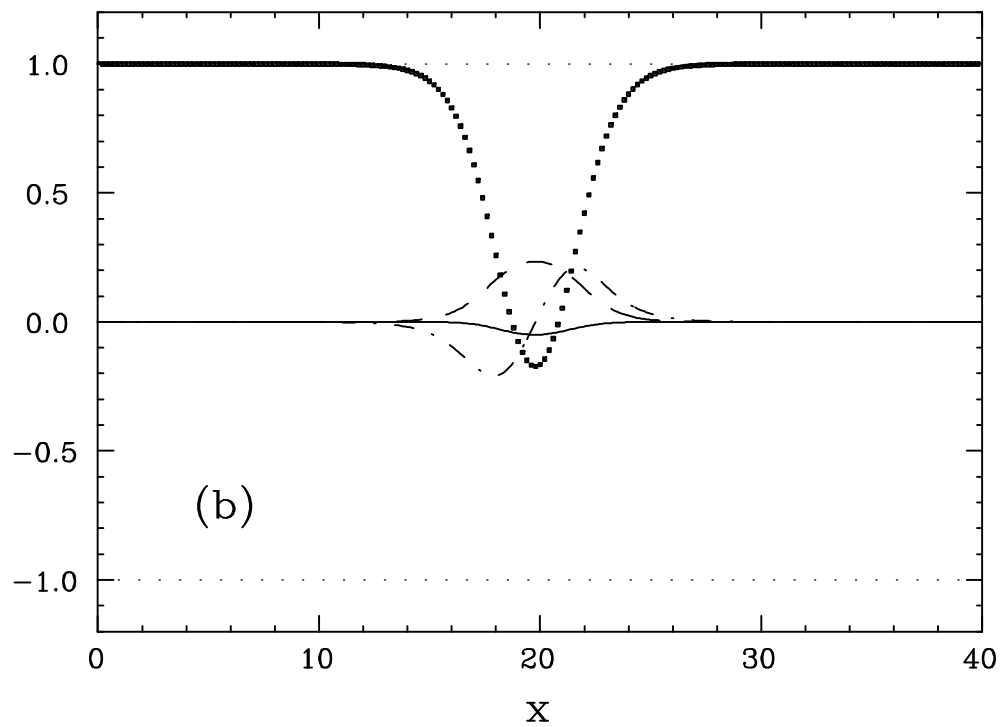


Fig.2

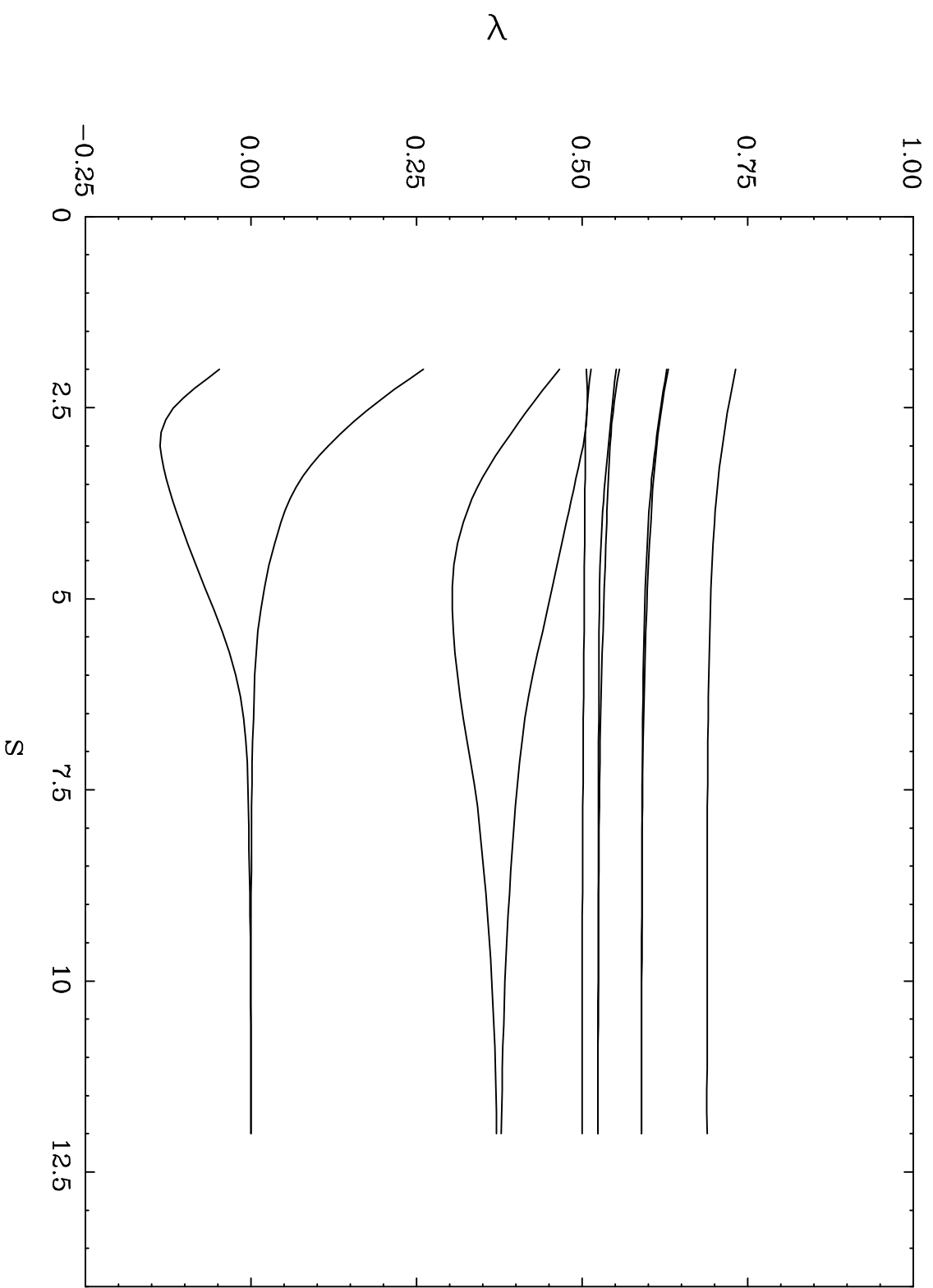


Fig.3

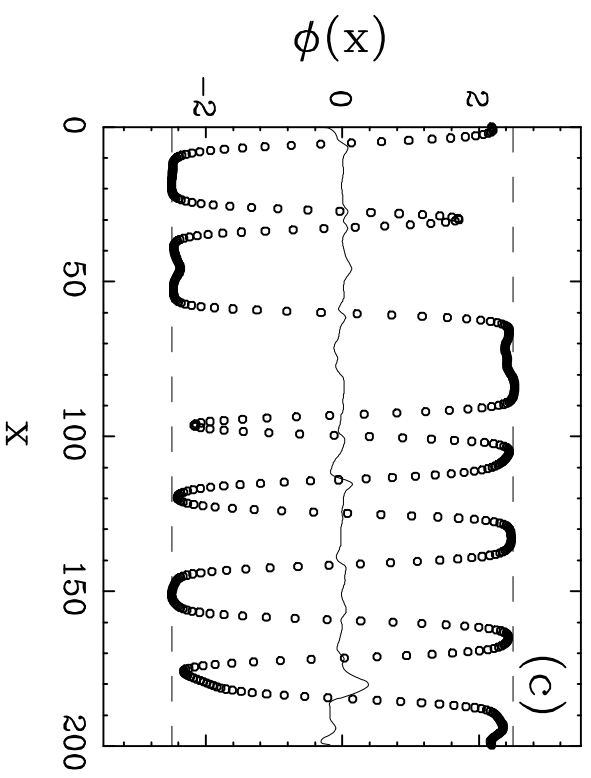
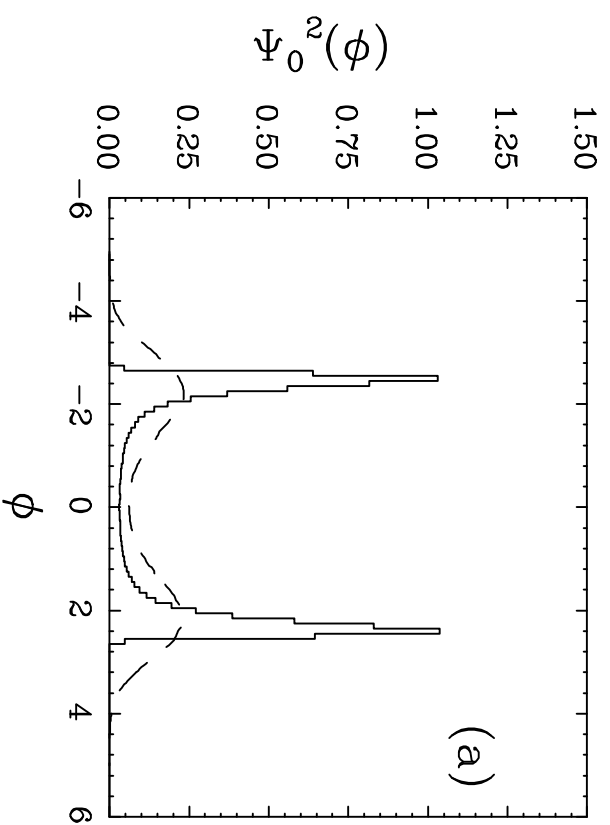
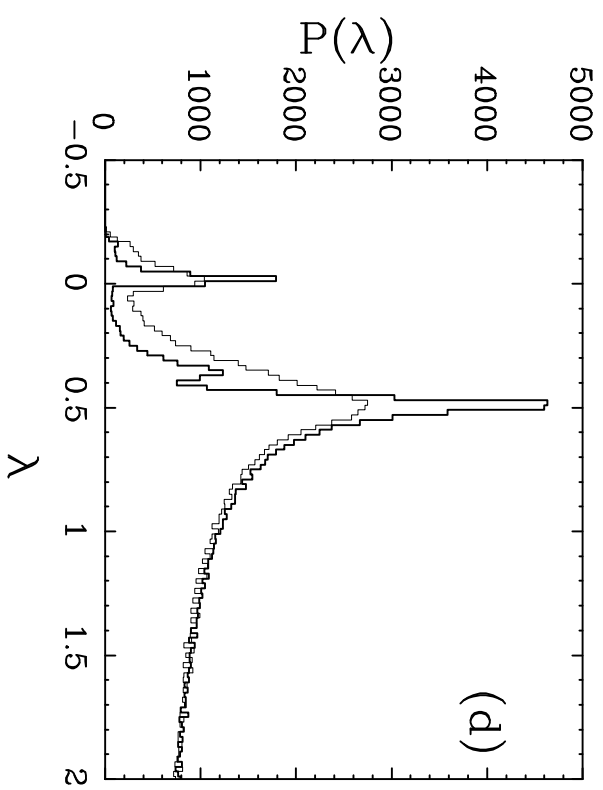
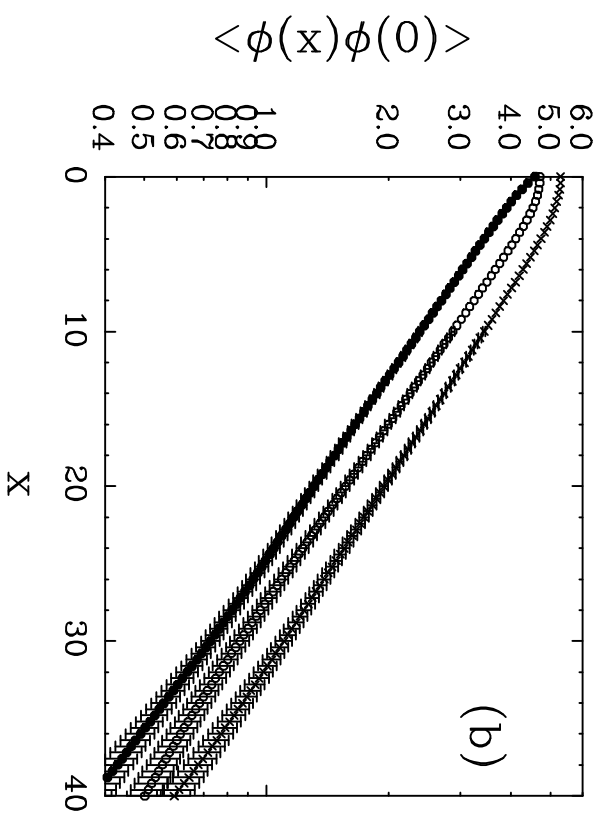
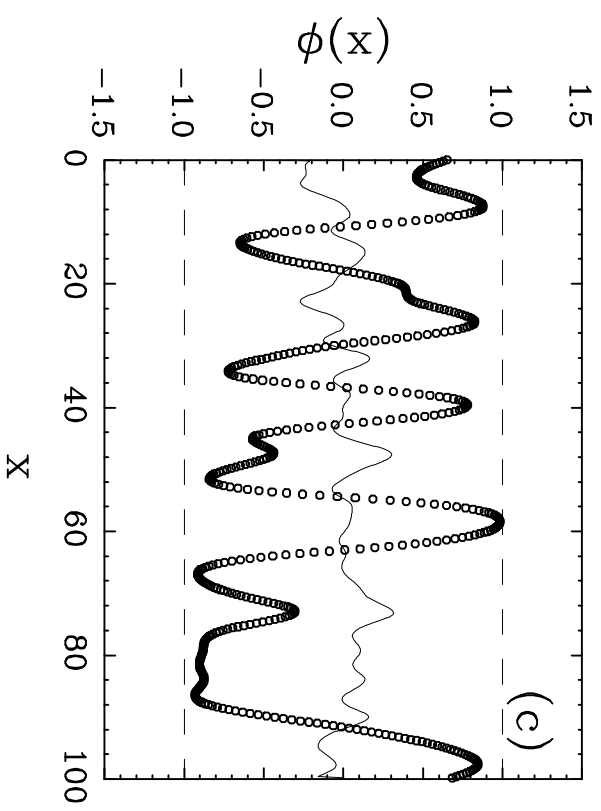
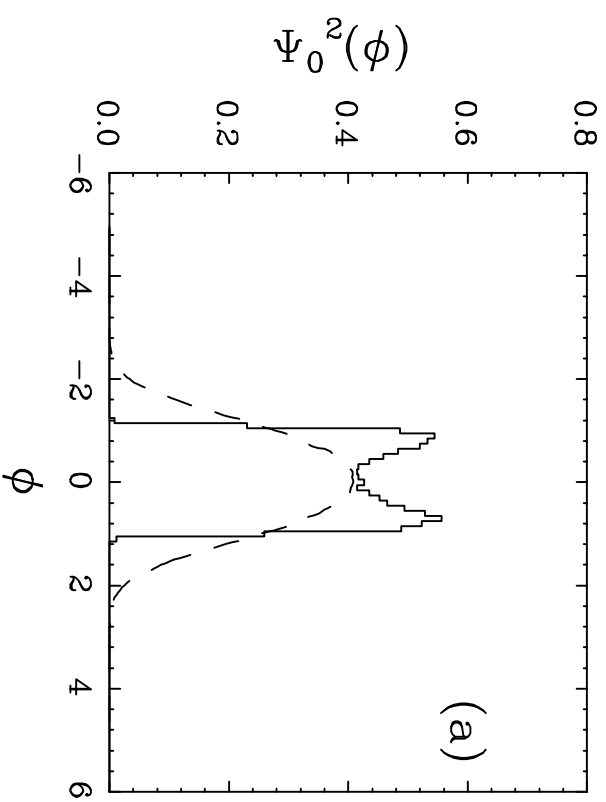
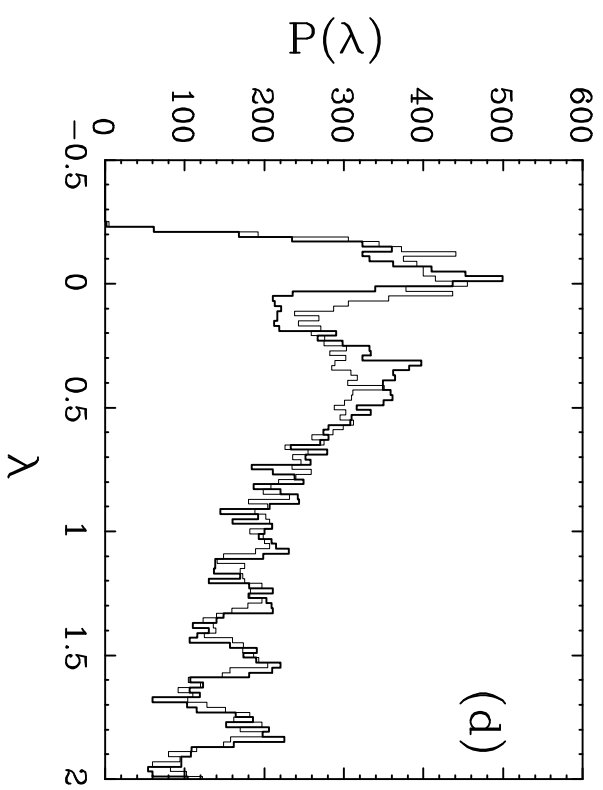
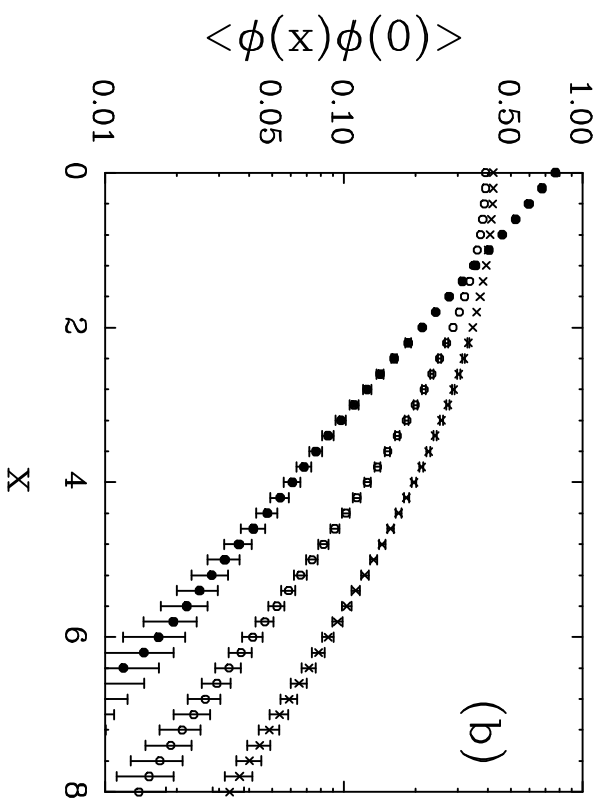


Fig.4



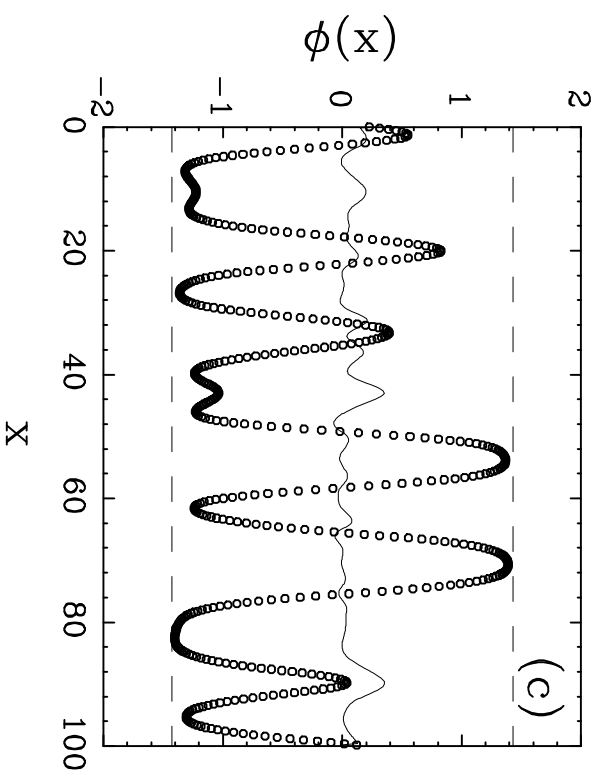
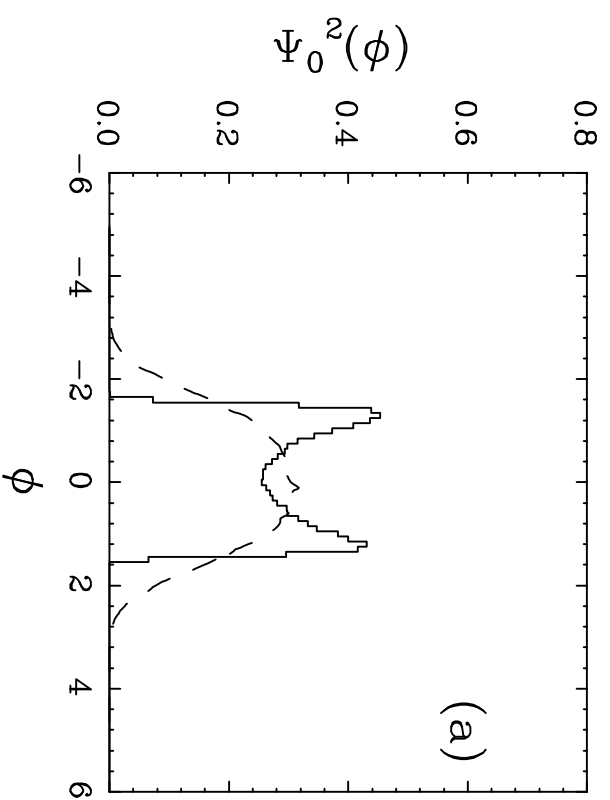
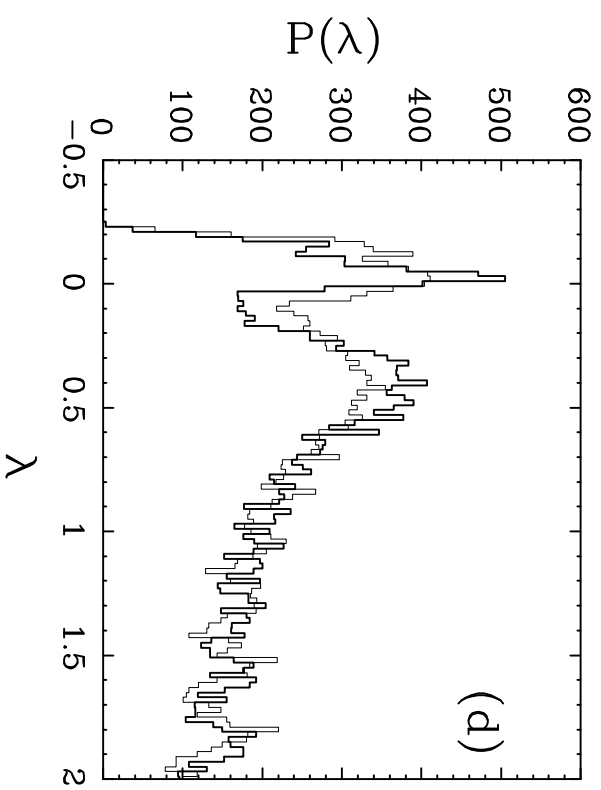
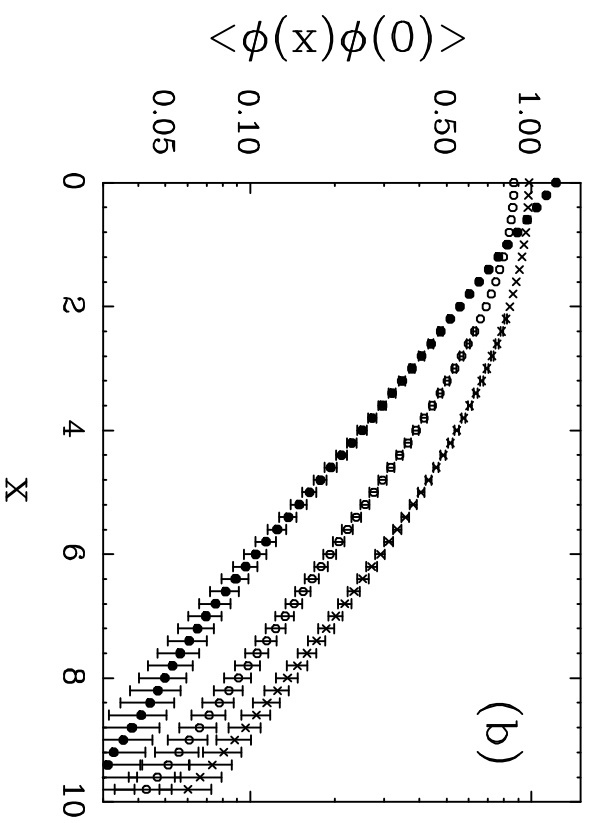


Fig.6

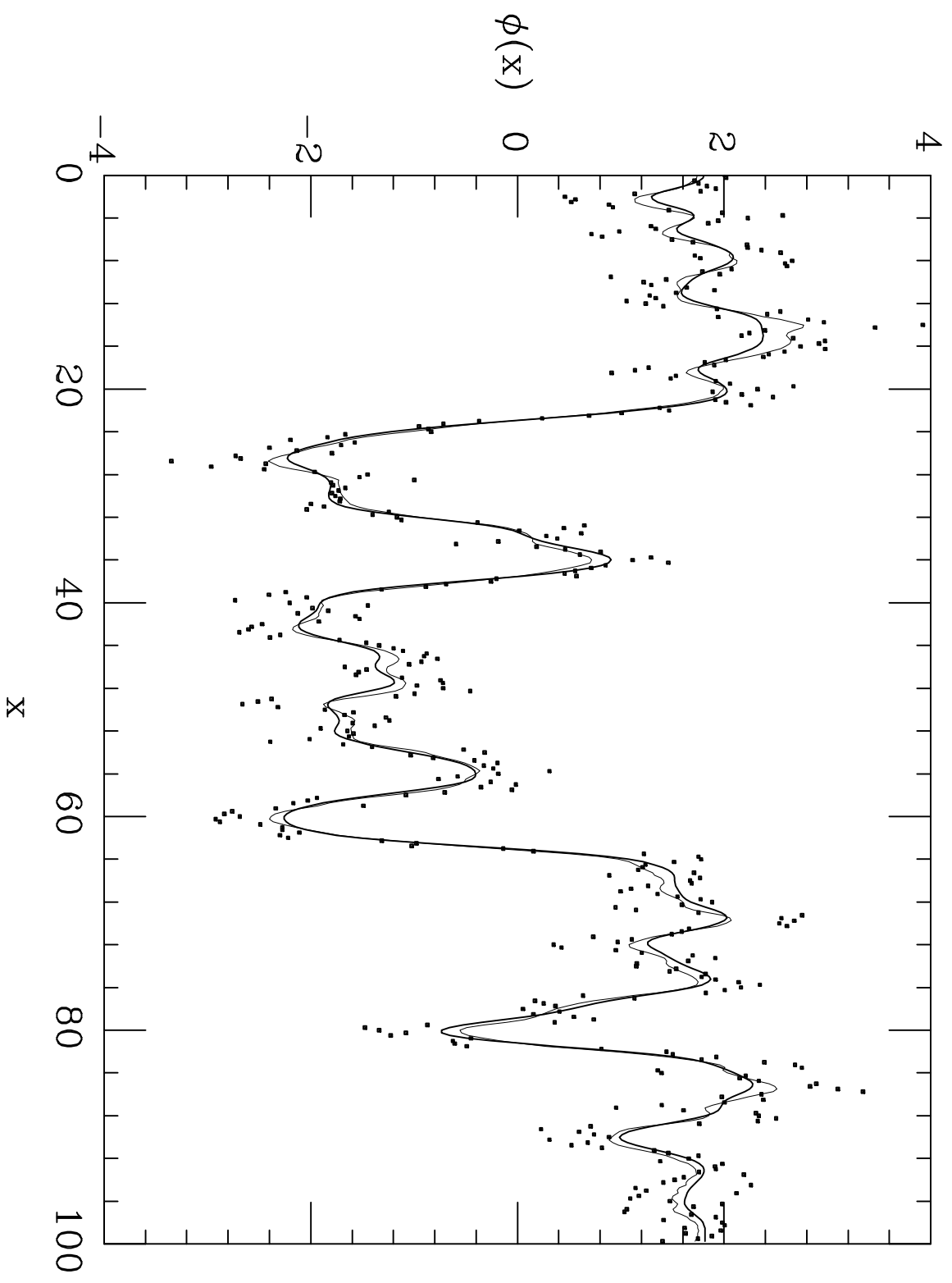


Fig. 7